PERGAMON

International Journal of Heat and Mass Transfer 45 (2002) 707–721

International Journal of HEAT and MASS TRANSFER

www.elsevier.com/locate/ijhmt

Distribution parameter and drift velocity of drift-flux model in bubbly flow

T. Hibiki [a,b,1], M. Ishii [c,*]

[a] Research Reactor Institute, Kyoto University, Kumatori, Sennan, Osaka 590-0494, Japan
[b] Graduate School of Engineering Science, Osaka University, Toyonaka, Osaka 560-8531, Japan
[c] School of Nuclear Engineering, Purdue University, West Lafayette, IN 47907-1290, USA

Received 4 December 2000; received in revised form 12 June 2001

Abstract

In view of the practical importance of the drift-flux model for two-phase flow analysis in general and in the analysis of nuclear-reactor transients and accidents in particular, the distribution parameter and the drift velocity have been studied for bubbly flow regime. The constitutive equation that specifies the distribution parameter in the bubbly flow has been derived by taking into account the effect of the bubble size on the phase distribution, since the bubble size would govern the distribution of the void fraction. A comparison of the newly developed model with various fully developed bubbly flow data over a wide range of flow parameters shows a satisfactory agreement. The constitutive equation for the drift velocity developed by Ishii has been reevaluated by the drift velocity calculated by local flow parameters such as void fraction, gas velocity and liquid velocity measured under steady fully developed bubbly flow conditions. It has been confirmed that the newly developed model of the distribution parameter and the drift velocity correlation developed by Ishii can also be applicable to developing bubbly flows.

Keywords: Drift-flux model; Distribution parameter; Drift velocity; Gas–liquid flow; Bubbly flow; Multiphase flow; Void fraction

1. Introduction

Two-phase flows always involve some relative motion of one phase with respect to the other; therefore, a two-phase-flow problem should be formulated in terms of two velocity fields. A general transient two-phase-flow problem can be formulated by using a two-fluid model [1,2] or a drift-flux model [3,4], depending on the degree of the dynamic coupling between the phases. In the two-fluid model, each phase is considered separately; hence the model is formulated in terms of two sets of conservation equations governing the balance of mass, momentum, and energy of each phase. However, an introduction of two momentum equations in a formulation, as in the case of the two-fluid model, presents considerable difficulties because of mathematical complications and of uncertainties in specifying interfacial–interaction terms between two phases [1,2]. Numerical instabilities caused by improper choice of interfacial–interaction terms in the phase-momentum equations are common; therefore careful studies on the interfacial constitutive equations are required in the formulation of the two-fluid model.

These difficulties associated with a two-fluid model can be significantly reduced by formulating two-phase problems in terms of the drift-flux model, in which the motion of the whole mixture is expressed by the mixture-momentum equation and the relative motion between phases is taken into account by a kinematic constitutive equation. Therefore, the basic concept of the drift-flux model is to consider the mixture as a whole, rather than as two separated phases. The formulation of the drift-flux model based on the mixture balance equations is simpler than the two-fluid model based on the separate balance equations for each phase. The most important

* Corresponding author. Tel.: +1-765-494-4587; fax: +1-765-494-9570.
E-mail addresses: hibiki@rri.kyoto-u.ac.jp (T. Hibiki), ishii@ecn.purdue.edu (M. Ishii).
[1] Tel.: +81-724-51-2373; fax: +81-724-51-2461.

0017-9310/02/$ - see front matter
PII: S0017-9310(01)00195-8

Nomenclature

A	cross-sectional area
a_i	interfacial area concentration
$\tilde{a}_i$	non-dimensional interfacial area concentration
C_0	distribution parameter
C_∞	asymptotic value of C_0
C_D	drag coefficient for a multi-particle system
$C_{D\infty}$	drag coefficient for a single particle
D	diameter of a pipe
D_H	hydraulic equivalent diameter of the flow channel
D_{max}	maximum spherical bubble diameter
D_{Sm}	Sauter mean diameter
F	quantity
g	gravitational acceleration
j	mixture volumetric flux
j_C	value of j at the channel center
j_f	superficial velocity of liquid phase
j_g	superficial velocity of gas phase
$j_{g,0}$	superficial velocity of gas phase at the inlet
Lo	Laplace length
$\widetilde{Lo}$	non-dimensional Laplace length
m	exponent
$N_{\mu f}$	viscosity number
n	exponent
P	pressure
R	radius of a pipe
r	radial distance
Re	Reynolds number
v_f	velocity of liquid phase
v_g	velocity of gas phase
V_{gj}	void-fraction-weighted mean drift velocity
v_{gj}	drift velocity of gas phase
v_r	relative velocity between phases
x_{WP}	radial position at the assumed square void peak
z	axial distance

Greek symbols

α	void fraction
α_C	value of α at the channel center
α_W	value of α at the wall
α_{WP}	value of α at the assumed square void peak
$\Delta\rho$	density difference between phases
ε	energy dissipation rate per unit mass
$\tilde{\varepsilon}$	non-dimensional energy dissipation rate per unit mass
μ_f	viscosity of liquid phase
μ_g	viscosity of gas phase
ν_f	kinematic viscosity of liquid phase
ρ_f	density of liquid phase
ρ_g	density of gas phase
ρ_m	density of mixture
σ	surface tension

Mathematical symbol

$\langle\rangle$	cross-sectional area average

assumption associated with the drift-flux model is that the dynamics of two phases can be expressed by the mixture-momentum equation with the kinematic constitutive equation specifying the relative motion between phases. The use of the drift-flux model is appropriate when the motions of two phases are strongly coupled.

The drift-flux model is an approximate formulation in comparison with the more rigorous two-fluid formulation. However, because of its simplicity and applicability to a wide range of two-phase-flow problems of practical interest, the drift-flux model is of considerable importance. In view of the practical importance of the drift-flux model for two-phase-flow analysis, the drift-flux model has been studied extensively. In the state-of-the-art, the constitutive equations for the drift-flux model have been developed well for vertical upward two-phase flows in conventional-diameter pipes (25–50 mm) under relatively high flow rate conditions [5]. The constitutive equations obtained under the conditions have been often used in computational thermohydraulic codes. The constitutive equations given by Zuber and Findley [3] or Ishii [4] have been used in the present system codes such as TRAC-P1A, CANAC-II, and ATHOS 3.

Recently, in order to meet the needs of improving the prediction accuracy in various two-phase-flow transient analyses, it has been required to develop precise constitutive equations for the distribution parameter and the drift velocity in various two-phase flows; for example, constitutive equations for:

1. low flow conditions [6],
2. counter-current flows and downward flows [6],
3. large diameter pipes [6,7], and
4. horizontal flows.

In addition to these, it would be important to develop or modify constitutive equations for bubbly flow regime. It is anticipated that the constitutive equation for the distribution parameter given by Ishii [4] may not give a good prediction in the bubbly flow regime. Wall peaking in void fraction distribution tends to decrease the distribution parameter considerably. In the mid-1970s, very few databases on local flow parameters were available and, therefore, it might be very difficult to include such local phenomena in the final constitutive equation. As local flow measurement techniques such as double sensor probe method [8] and hotfilm anemometry [9] have been developed, databases of local flow parameters for gas and liquid phases in the bubbly flow have been

developed extensively [10–17]. This enables reassessment of the constitutive equations for the distribution parameter and the drift velocity by using the local flow parameters such as void fraction, gas velocity, and liquid velocity. In view of this, this study focuses on the development of the constitutive equation for the distribution parameter in bubbly flows, and the reevaluation of the constitutive equation for the drift velocity given by Ishii [4] by using the measured local flow parameters.

2. One-dimensional drift-flux model

2.1. Formulation of one-dimensional drift-flux model

The drift-flux model is one of the most practical and accurate models for two-phase flow. The model takes into account the relative motion between phases by a constitutive relation. It has been utilized to solve many engineering problems involving two-phase flow dynamics [5]. In particular, its application to forced convection systems has been quite successful. In what follows, the one-dimensional drift-flux model will be derived by averaging the local drift velocity over the channel cross-section [3,4]. The rational approach to obtain a one-dimensional model is to integrate the three-dimensional model over a cross-sectional area and then to introduce proper mean values.

The drift velocity of a gas phase, v_{gj}, is defined as the velocity of the gas phase, v_g, with respect to the volume center to the mixture, j:

$$v_{gj} = v_g - j = (1-\alpha)(v_g - v_f) = (1-\alpha)v_r, \tag{1}$$

where α, v_f, and v_r are the void fraction, the liquid velocity, and the relative velocity between phases, respectively. The void-fraction-weighted mean drift velocity is given by

$$\frac{\langle \alpha v_{gj}\rangle}{\langle\alpha\rangle} = \frac{\langle \alpha v_g\rangle}{\langle\alpha\rangle} - \frac{\langle \alpha j\rangle}{\langle\alpha\rangle} = \frac{\langle j_g\rangle}{\langle\alpha\rangle} - \frac{\langle \alpha j\rangle}{\langle\alpha\rangle}, \tag{2}$$

where a simple area average of a quantity, F, over the cross-sectional area, A, is defined by

$$\langle F\rangle = \frac{1}{A}\int_A F\,\mathrm{d}A. \tag{3}$$

The one-dimensional drift-flux model can be derived by recasting Eq. (2) as

$$\frac{\langle j_g\rangle}{\langle\alpha\rangle} = \frac{\langle \alpha j\rangle}{\langle\alpha\rangle\langle j\rangle}\langle j\rangle + \frac{\langle \alpha v_{gj}\rangle}{\langle\alpha\rangle} = C_0\langle j\rangle + V_{gj}, \tag{4}$$

where C_0 and V_{gj} are the distribution parameter defined by Eq. (5) and the void-fraction-weighted mean drift velocity defined by Eq. (6), respectively.

$$C_0 \equiv \frac{\langle \alpha j\rangle}{\langle\alpha\rangle\langle j\rangle}, \tag{5}$$

and

$$V_{gj} \equiv \frac{\langle \alpha v_{gj}\rangle}{\langle\alpha\rangle}. \tag{6}$$

The void-fraction-weighted mean gas velocity, $\langle j_g\rangle/\langle\alpha\rangle$, and the cross-sectional mean mixture volumetric flux, $\langle j\rangle$, are easily obtainable parameters in experiments. Therefore, Eq. (4) suggests a plot of $\langle j_g\rangle/\langle\alpha\rangle$ versus $\langle j\rangle$. An important characteristic of such a plot is that, for two-phase flow regimes with fully developed void and velocity profiles, the data points cluster around a straight line. The value of the distribution parameter, C_0, has been obtained indirectly from the slope of the line, whereas the intercept of this line with the void-fraction-weighted mean gas velocity axis can be interpreted as the void-fraction-weighted mean local drift velocity, V_{gj}. As recent development of local sensor techniques [8,9,18] enables the measurement of the local flow parameters in a bubbly flow such as void fraction, and gas and liquid velocities, the values of C_0 and V_{gj} in a bubbly flow can be determined directly by Eqs. (5) and (6) from experimental data of the local flow parameters.

2.2. Analytical prediction of distribution parameter

The value of C_0 can be estimated from assumed profiles of the void fraction, α, and the mixture volumetric flux, j. By assuming power-law profiles in a pipe for j and α, we have

$$\frac{j}{j_C} = 1 - \left(\frac{r}{R}\right)^m, \tag{7}$$

$$\frac{\alpha-\alpha_W}{\alpha_C-\alpha_W} = 1 - \left(\frac{r}{R}\right)^n, \tag{8}$$

where j_C, α_C, α_W, r, and R are, respectively, the values of j and α at the channel center, the value of α at the wall, the radial distance, and the radius of pipe. Since the void fraction at the wall is 0 for adiabatic flows and the gas velocity at the wall is presumably about 0 for boiling flows, the value of j ($= v_g\alpha$) at the wall is assumed to be 0 in Eq. (7). m and n are the exponents. By substituting these profiles into the definition of C_0 given by Eq. (5), we obtain

$$C_0 = 1 + \frac{2}{m+n+2}\left(1 - \frac{\alpha_W}{\langle\alpha\rangle}\right). \tag{9}$$

On the other hand, by assuming an extreme wall-peaked profile in a pipe for α (see Fig. 1(b)), we have

$$\begin{aligned} &\alpha = \alpha_{WP}, \quad x_{WP} \leqslant \frac{r}{R} \leqslant 1, \\ &\alpha = 0, \quad 0 \leqslant \frac{r}{R} \leqslant x_{WP}, \end{aligned} \tag{10}$$

where α_{WP} and x_{WP} are the void fraction and the radial position at the assumed square void peak, respectively.

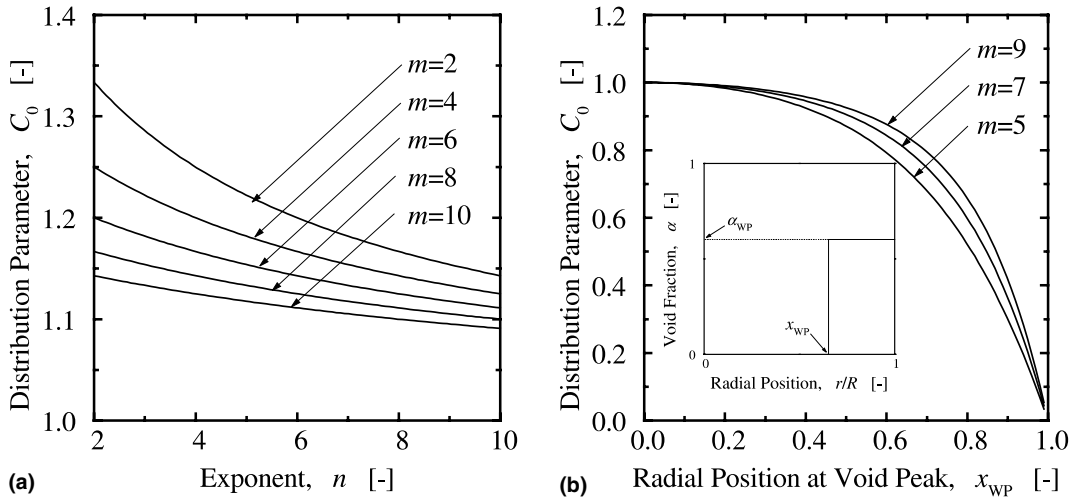

Fig. 1. Analytical predictions of distribution parameters. (a) Power-law profile in a pipe for α, (b) wall-peaked profile in a pipe for α.

By substituting the profiles given by Eqs. (7) and (10) into the definition of C_0 given by Eq. (5), we obtain

$$C_0 = \frac{m - x_{WP}^2\{(m+2) - 2x_{WP}^m\}}{m(1+x_{WP})(1-x_{WP})}. \tag{11}$$

Figs. 1(a) and (b) show the distribution parameters calculated by Eq. (9) for an adiabatic two-phase flow ($\alpha_W = 0$), and Eq. (11), respectively. For the power-law profiles for j and α, the value of the distribution parameter is always larger than unity, whereas for the extreme wall-peaked profile for α, the value of the distribution parameter is always smaller than unity. The steep wall peaking tends to decrease the distribution parameter considerably. In addition, if the concentration profile is uniform across the channel, then the value of the distribution parameter is equal to unity.

2.3. Constitutive equations of distribution parameter and drift velocity in bubbly flow

Ishii [4] developed a simple correlation for the distribution parameter in bubbly flow regime. Ishii first considered a fully developed bubbly flow and assumed that C_0 would depend on the density ratio, ρ_g/ρ_f, and on the Reynolds number, Re. As the density ratio approaches unity, the distribution parameter C_0 should become unity. Based on the limit and various experimental data in fully developed flows, the distribution parameter was given approximately by

$$C_0 = C_\infty(Re) - \{C_\infty(Re) - 1\}\sqrt{\rho_g/\rho_f}, \tag{12}$$

where C_∞ is the asymptotic value of C_0. Here, the density group scales the inertia effects of each phase in a transverse void distribution. Physically, Eq. (12) models the tendency of the lighter phase to migrate into a higher-velocity region, thus resulting in a higher void concentration in the central region [4]. For a laminar flow, C_∞ is 2, but due to the large velocity gradient, C_0 is very sensitive to $\langle\alpha\rangle$ at low void fractions [4].

Based on a wide range of Reynolds numbers, Ishii approximated C_∞ to be 1.2 for a flow in a pipe [4]. Thus, for a fully developed turbulent bubbly flow in a pipe

$$C_0 \cong 1.2 - 0.2\sqrt{\rho_g/\rho_f}. \tag{13}$$

In two-phase systems with heat addition, the change of void profiles from concave to convex can occur. The concave void fraction profile is caused by the wall nucleation and delayed transverse migration of bubbles toward the center of a channel. Under these conditions, most of the bubbles are initially located near the nucleating wall. The concave profile is particularly pronounced in the subcooled boiling regime, because here only the wall-boundary layer is heated above the saturation temperature and the core liquid is subcooled. This temperature profile will induce collapses of migrating bubbles in the core region and resultant latent heat transport from the wall to the subcooled liquid. However, a similar concave profile can also be obtained by injecting gas into flowing liquid through a porous tube wall.

For a flow with generation of void at the wall due to either nucleation or gas injection, the distribution parameter C_0 should have a near-zero value at the beginning of the two-phase flow region. With the increase in the cross-sectional mean void fraction, the peak of the local void fraction moves from the near-wall region to the central region. This will lead to the increase in the value of C_0 as the void profile develops. In view of the

basic characteristics described above and various experimental data, Ishii [4] proposed the following simple correlation.

$$C_0 = \left(1.2 - 0.2\sqrt{\rho_g/\rho_f}\right)(1 - e^{-18\langle\alpha\rangle}). \quad (14)$$

This expression indicates the significance of the developing void profile in the region given by $0 < \langle\alpha\rangle < 0.25$; beyond this region, the value of C_0 approaches rapidly to that for a fully developed flow.

Ishii [4] also developed a simple correlation for the drift velocity in bubbly flow regime. In the distorted-fluid-particle regime, the single particle drag coefficient, $C_{D\infty}$, depends only on the particle radius and fluid properties and not on the velocity or the viscosity. Thus, for a particle of a fixed diameter, $C_{D\infty}$ becomes constant. In considering the drag coefficient, C_D, for a multi-particle system with the same radius, it is necessary to take into account the restrictions imposed by the existence of other particles in the flow field. Therefore, C_D is expected to be different from $C_{D\infty}$, in this regime. Because of the wake characteristic of the turbulent eddies and particle motions, a particle sees the increased drag due to other particles in essentially similar ways as in Newton's regime for a solid-particle system, where $C_{D\infty}$ is also constant under a wake turbulent flow condition. Hence, Ishii [4] postulated that regardless of the differences in $C_{D\infty}$ in these regimes, the effect of increased drag in the distorted-fluid-particle regime could be predicted by a similar expression as that in Newton's regime. In other words, Ishii [4] assumed that $C_D/C_{D\infty}$ for the distorted particle regime would be the same as that in Newton's regime. Under this assumption, the drift velocity for the distorted-fluid-particle or bubbly flow can be obtained as [4]

$$V_{gj} = \sqrt{2}\left(\frac{g\sigma\Delta\rho}{\rho_f^2}\right)^{1/4}(1 - \langle\alpha\rangle)^{1.75} \quad \text{for } \mu_f \gg \mu_g. \quad (15)$$

where g, σ, $\Delta\rho$, μ_f and μ_g are the gravitational acceleration, the surface tension, the density difference between phases, the liquid viscosity and the gas viscosity, respectively.

3. Results and discussion

3.1. Databases used for determination of distribution parameter and drift velocity

In order to determine the distribution parameter and the drift velocity experimentally, the present authors measured local flow parameters of adiabatic air–water bubbly flows in vertical pipes with inner diameters, D, of 25.4 and 50.8 mm at the Thermal-hydraulics and Reactor Safety Laboratory in Purdue University [15–17]. Local measurements of void fraction and gas velocity were performed by using the double sensor probe method [15]. On the other hand, local measurement of liquid velocity was conducted by using hotfilm anemometry [15]. Data were taken at three different axial locations as well as 15 radial positions. For $D = 25.4$ mm, a total of 75 ($=25 \times 3$) data sets were acquired consisting of 25 flow conditions [17], and for $D = 50.8$ mm, a total of 54 ($=18 \times 3$) data sets were acquired consisting of 18 flow conditions [16]. The detailed discussions of local flow parameters are found in our previous papers [16,17]. In addition to our databases, four databases listed in Table 1 are also available. These databases [10–13] include local parameters such as void fraction, gas velocity, and liquid velocity. The detailed experimental conditions are shown in Table 1. A total of 214 data sets are available to determine the distribution parameter and the drift velocity experimentally.

3.2. Phase distribution pattern map

Serizawa and Kataoka [19] roughly classified the phase distribution patterns into four basic types of the phase distributions, that is, wall peak, intermediate peak (broad wall peak), core peak, and transition (two peaks at the channel center and wall). As an example, Fig. 2(a) shows maps of phase distribution patterns measured at $z/D = 53.5$ for $D = 50.8$ mm in our previous experiment [16]. In addition to the above four basic patterns of the phase distributions, "flat" distribution was observed for $\langle j_f\rangle = 5.00$ m/s and $\langle\alpha\rangle < 0.15$. The open symbols of circle, triangle, reversed triangle, square, and diamond in the figure indicate the wall peak, the transition, the intermediate peak, the core peak, and the flat, respectively. In Fig. 2, the solid and broken lines, respectively, are the flow regime transition boundaries predicted by the model of Taitel et al. [20], and phase distribution pattern transition boundaries, which were developed by Serizawa and Kataoka [19] based on experiments performed by different researchers with different types of bubble injections in round tubes ($20\text{ mm} \leqslant D \leqslant 86.4$ mm). A fairly good agreement is obtained between Serizawa–Kataoka's map [19] and the phase distribution patterns observed in our previous experiment [16].

Fig. 2(b) shows the values of the distribution parameter determined experimentally from the measured local flow parameters. The solid symbols of circle, triangle, reversed triangle, and square indicate the values of the distribution parameter such as $C_0 < 1.00$, $1.00 \leqslant C_0 < 1.05$, $1.05 \leqslant C_0 < 1.10$, and $1.10 \leqslant C_0$, respectively. Even though a flow regime can be categorized as a bubbly flow, the distribution parameter appears not to have a unique value as expressed by Eq. (13). This suggests the necessity of the development of the con-

Table 1
Databases used in this study

Investigators	Geometry and size (mm)	Flow direction	Gas	Liquid	z/D (dimensionless)	Pressure (MPa)	Superficial gas velocity (m/s)	Superficial liquid velocity (m/s)	Bubble Sauter mean diameter (mm)	Number of data	Technique
Hibiki and Ishii [17]	25.4 ID pipe	Vertical	Air	Water	12	0.10	0.0473–1.12	0.262–3.49	1.72–3.99	25	Probe
					65		0.0257–1.03	0.262–3.49	2.19–4.10	25	
					125		0.056–1.27	0.262–3.49	2.05–3.99	25	
Hibiki et al. [16]	50.8 ID pipe	Vertical	Air	Water	6	0.10	0.0257–4.45	0.491–5.00	1.40–3.31	18	Probe
					30		0.0328–4.39	0.491–5.00	1.78–3.52	18	
					54		0.0257–4.88	0.491–5.00	1.77–3.86	18	
Grossetete [13]	38.1 ID pipe	Vertical	Air	Water	8	0.10	0.0487–0.395	0.526–0.877	2.28–3.91	7	Probe
					55		0.0596–0.444	0.526–0.877	2.75–11.7	6	
					155		0.0840–0.572	0.526–0.877	3.50–34.5	7	
Kalkach-Navarro [12]	38.1 ID pipe	Vertical	Air	Water	50	0.10	0.0655–0.343	0.30–1.25	3.35–5.46	17	Probe
Serizawa et al. [11]	60.0 ID pipe	Vertical	Air	Water	30	0.10	0.0941–0.416	0.442–1.03	3.03–7.75	6	Probe
Liu [10]	38.1 ID pipe	Vertical	Air	Water	36	0.10	0.0197–0.353	0.376–1.39	2.12–4.26	42	Probe

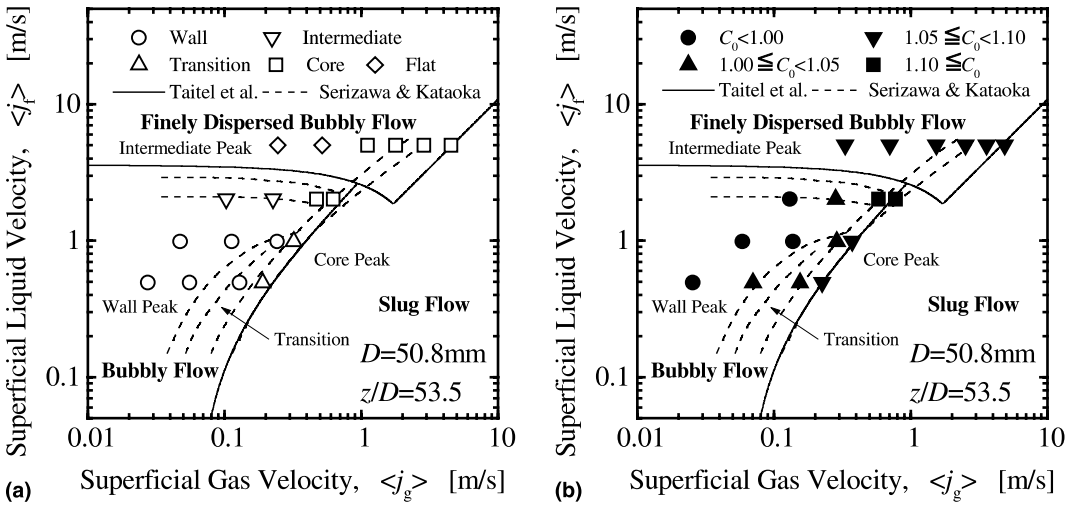

Fig. 2. A map of phase distribution patterns. (a) Phase distribution pattern map, (b) distribution parameters corresponding to the phase distribution patterns.

stitutive equation for the distribution parameter in bubbly flow.

3.3. Development of constitutive equation for distribution parameter

As discussed in Section 2.3, Eq. (13) physically models the tendency of the lighter phase to migrate into a higher-velocity region, thus resulting in a higher void concentration in the central region. As can be seen from Fig. 2(b), Eq. (13) would not give a good prediction of the distribution parameter in a flow region where the wall peak in void distribution appears. Before modification of Eq. (13), the distribution parameters obtained by measured local flow parameters in our previous experiments [16,17] are compared with Eqs. (13) and (14) developed for a flow with generation of void at the wall as shown in Fig. 3. The solid and broken lines in Fig. 3 indicate the distribution parameters calculated by Eqs. (14) and (13), respectively. Eq. (14) as well as Eq. (13) does not agree with the experimental distribution parameters satisfactorily. The deviations between Eq. (14) and the experimental distribution parameters are marked particularly for low void fraction range. For a wall nucleation case assumed in the derivation of Eq. (14), tiny bubbles would exist only at the channel wall, resulting in a near-zero value of the distribution parameter (see Fig. 1(b)). However, in our previous

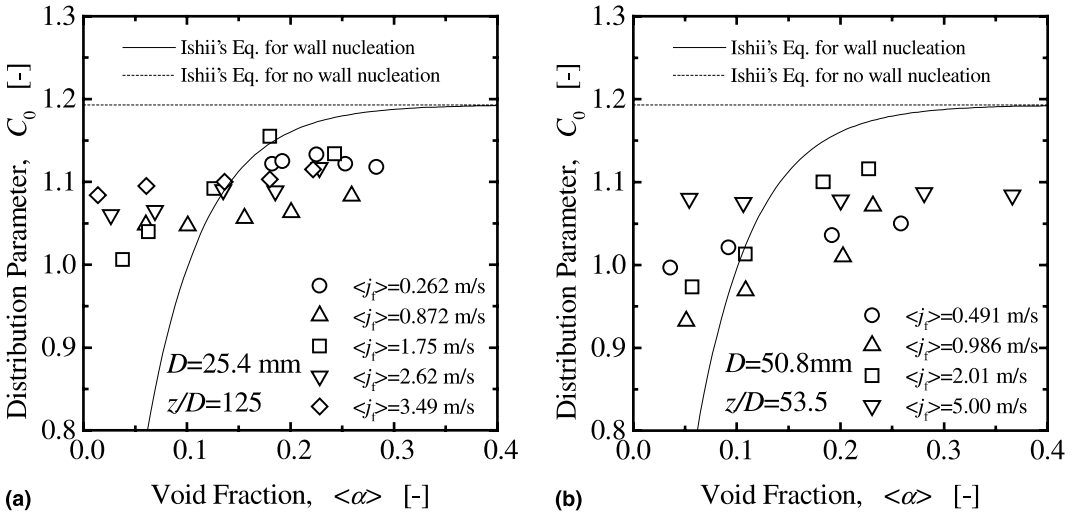

Fig. 3. Comparison of Ishii's model for distribution parameter in nucleate boiling flow with distribution parameters determined experimentally. (a) Experiment using a 25.4 mm-diameter pipe [17], (b) experiment using a 50.8 mm-diameter pipe [16].

experiments for adiabatic air–water bubbly flows [16,17], the bubble diameter is a few millimeters, and the bubbles are distributed in various patterns such as the wall peak, the transition, the intermediate peak, the core peak, and the flat as shown in Fig. 2(a) even for the low void fraction range. Thus, at the low void fraction range, the wall peaking in the adiabatic flow is much smaller than that in the boiling flow. This results in the value of the distribution parameter being much higher than the prediction by Eq. (14) at the low void fraction region. Fig. 3 also suggests that the void fraction may not be a dominant factor to determine the distribution parameter in the bubbly flow regime. Thus, although Eq. (14) is applicable to nucleate boiling flow, it cannot describe the wall peaking phenomena in adiabatic bubbly flows. It should be noted here that the wall peaking appears to persist at the higher void fraction ($\langle\alpha\rangle > 0.2$) in our adiabatic data (see Figs. 2(a) and 5).

Sekoguchi et al. [21] observed the behaviors of isolated bubbles, which were introduced into vertical water flow in a 25 mm × 50 mm rectangular channel through a single nozzle. Based on their observations, they found that the bubble behaviors in dilute suspension flow might depend on the bubble size and the bubble shape. In their experiment, only distorted ellipsoidal bubbles with a diameter smaller than nearly 5 mm tended to migrate toward the wall, whereas distorted ellipsoidal bubbles with a diameter larger than 5 mm and spherical bubbles rose in the channel center. On the other hand, for the water velocity lower than 0.3 m/s, no bubbles were observed in the wall region.

Zun [22] also obtained a similar result. He performed an experiment to study the void fraction radial profiles in upward vertical bubbly flow at very low average void fractions, around 0.5%. In his experiment, the wall void peaking flow regime existed both in laminar and turbulent bulk liquid flows. The experimental results on turbulent bulk liquid flow at Reynolds number near 1000 showed distinctive higher bubble concentration at the wall region if the bubble equivalent sphere diameter appeared in the range between 0.8 and 3.6 mm. Intermediate void profiles were observed at bubble sizes either between 0.6 and 0.8 mm or 3.6 and 5.1 mm. Bubbles smaller than 0.6 mm or larger than 5.1 mm tended to migrate towards the channel center. Thus, these experimental results suggest that the bubble size plays a dominant role in void fraction profiles.

Serizawa and Kataoka [19] also gave an extensive review on the bubble behaviors in bubbly flow regime. Recently, Tomiyama et al. [23] conducted experiments and numerical simulations on lateral migration of a single bubble in stagnant liquids and laminar flows to examine the effects of the Eötvös number and dimensionless liquid volumetric flux on lateral forces. They confirmed that (1) a lateral force due to the existence of the wall acted on a near-wall bubble and (2) a lift force due to the net circulation of liquid around a bubble strongly depended on the Eötvös number. To extend the above observations to dense suspension flow such as turbulent bubbly flow with high void fraction, some further studies should be indispensable. For example, the relationship between the channel size and the threshold diameter to determine the direction of the bubble movement should be addressed. If the bubble size were comparable to the channel size, even bubbles with a diameter smaller than 5 mm would rise in the channel center, resulting in a core void peaking.

Based on the above discussions, it is anticipated that the bubble size would affect the void distribution as well as the distribution parameter. In addition to this, the change of the mixture-volumetric-flux profile due to the introduction of bubbles would vary the distribution parameter. It has been known that the introduction of bubbles into the liquid flow flattens the liquid-velocity profile with a relatively steep decrease close to the wall particularly for $\langle j_f\rangle < 1.0$ m/s [17]. However, as can be seen from Fig. 1, a slight change of the mixture-volumetric-flux profile may not affect the distribution parameter significantly. Thus, the key parameter determining the distribution parameter would be the bubble size. Taking account of the bubble size to the channel size, the distribution parameters determined by local flow parameters measured under steady fully developed turbulent bubbly flow conditions are plotted against the non-dimensional Sauter mean diameter, $\langle D_{Sm}\rangle/D$, in Fig. 4. The distribution parameter steeply increases with the bubble diameter at the small $\langle D_{Sm}\rangle/D$ range, and approaches to an asymptotic value given by Eq. (13). In

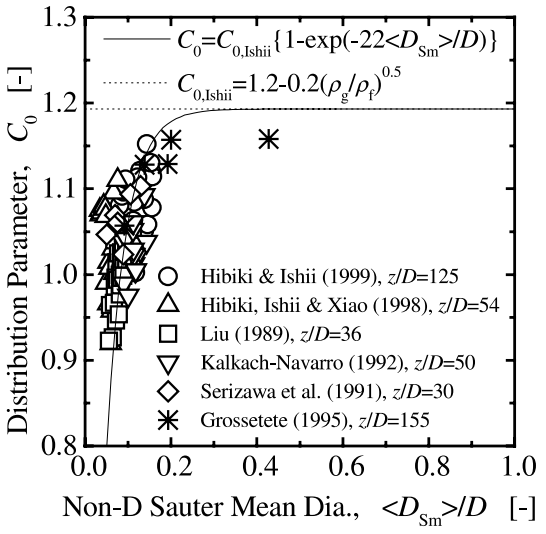

Fig. 4. Comparison of newly developed model for distribution parameter in bubbly flow regime with distribution parameters determined experimentally.

view of the basic characteristics described above and various experimental data, the following simple correlation is proposed:

$$C_0 = \left(1.2 - 0.2\sqrt{\rho_g/\rho_f}\right)\left(1 - e^{-22\langle D_{Sm}\rangle/D}\right). \quad (16)$$

Here, the coefficient of $\langle D_{Sm}\rangle/D$ ($= -22$) has been determined by the databases with the least-square method. The solid and broken lines are the distribution parameters calculated by Eqs. (16) and (13), respectively. Eq. (16) indicates the significance of the developing void profile in the region given by $0 < \langle D_{Sm}\rangle/D < 0.2$; beyond this region, the values of C_0 approach rapidly to that for a core peak. The modified correlation of the distribution parameter, Eq. (16), agrees with the distribution parameters determined by local flow parameters measured under fully developed turbulent bubbly flow conditions within an average relative deviation of $\pm 6.7\%$. The applicability of Eq. (16) is confirmed for 115 data sets taken under the experimental conditions such as $0.262\ \text{m/s} \leqslant \langle j_f\rangle \leqslant 5\ \text{m/s}$, $25.4\ \text{mm} \leqslant D \leqslant 60\ \text{mm}$, and $1.40\ \text{mm} \leqslant \langle D_{Sm}\rangle$.

As already mentioned, it may be anticipated that spherical bubbles tend to migrate toward the channel center resulting in core void peak. The applicability of Eq. (16) would be limited by the following maximum spherical bubble diameter [24]:

$$D_{max} = 4\sqrt{\frac{2\sigma}{g\Delta\rho}}N_{\mu f}^{1/3}, \quad (17)$$

where $N_{\mu f}$ is the viscosity number defined by

$$N_{\mu f} = \frac{\mu_f}{(\rho_f\sigma\sqrt{\sigma/g\Delta\rho})^{1/2}}. \quad (18)$$

The maximum spherical bubble diameter for air–water system at atmospheric pressure and 20°C is estimated to be 2 mm from Eq. (17). It may be concluded from Zun's observation [22] and the results in this study that Eq. (16) can practically be applicable to the condition of $\langle D_{Sm}\rangle \geqslant D_{max}/3$.

As for the applicability of Eq. (16) to low liquid flow systems, it may be anticipated that the prediction accuracy of the distribution parameter by Eq. (16) would decrease due to the tendency of bubble migration towards the channel center for low liquid flow rate. However, for such low liquid flow systems, the orders of magnitude of the distribution parameter effect and of the local slip effect are about the same. Thus, in calculating a void fraction, the value of the distribution parameter is not as critical as in a forced convection system with high liquid flow rate where often the distribution parameter is the dominant factor because of large values of the mixture volumetric flux. However, for a general correlation, it is necessary to model the distribution parameter more accurately. It should also be noted here that a secondary flow induced at low flow rate in a large diameter pipe may affect the distribution parameter significantly [7,25–27]. The applicability of Eq. (16) to the large diameter pipe ($D > 60$ mm) or the development of new correlation for the distribution parameter in the large diameter pipe should be addressed in a future study.

For a practical use, the Sauter mean diameter in Eq. (16) should be correlated with easily measurable quantities such as superficial gas and liquid velocities. Recently, the correlation of the interfacial area concentration under steady fully developed bubbly flow conditions has been developed based on the interfacial area transport equation as follows [28]:

$$\langle\tilde{a}_i\rangle = 0.500\tilde{Lo}^{-0.283}\langle\alpha\rangle^{0.847}\langle\tilde{\varepsilon}\rangle^{0.283}, \quad (19)$$

where

$$\langle\tilde{a}_i\rangle \equiv \frac{\langle a_i\rangle}{Lo^{-1}}, \quad Lo \equiv \sqrt{\frac{\sigma}{g\Delta\rho}}, \quad \tilde{Lo} \equiv \frac{Lo}{D_H}$$

and $$\langle\tilde{\varepsilon}\rangle \equiv Lo\left(\frac{\langle\varepsilon\rangle}{v_f^3}\right)^{1/4}.$$

The energy dissipation rate per unit mass in Eq. (19) can be simply calculated from the mechanical energy equation as [29,30]:

$$\langle\varepsilon\rangle = \frac{\langle j\rangle}{\rho_m}\left(-\frac{dP}{dz}\right)_F, \quad (20)$$

where ρ_m, and $(-dP/dz)_F$ refer to the mixture density, and the pressure loss per unit length due to friction, respectively. The pressure loss per unit length due to friction can be calculated from Lockhart–Martinelli's correlation [31]. The above interfacial area correlation, Eq. (19), agreed with 204 data sets measured in air–water bubbly flows under various conditions such as channel geometry (circular or rectangular channel), flow direction (vertical or horizontal flow), superficial gas velocity (0.018–4.87 m/s), and superficial liquid velocity (0.262–6.55 m/s) within an average relative deviation of $\pm 11.1\%$.

The Sauter mean diameter can be calculated by using Eq. (19) and the relationship of $\langle D_{Sm}\rangle = 6\langle\alpha\rangle/\langle a_i\rangle$. As a consequence, the distribution parameter is given as a function of flow parameters such as void fraction, and superficial gas and liquid velocities.

3.4. Axial development of distribution parameter

Fig. 5 shows examples of the axial development of the void fraction profiles observed in our previous experiment using a pipe with $D = 50.8$ mm [16]. The upper and lower data were measured at $z/D = 6.00$ and 53.5, respectively. Fig. 6 shows the axial development of

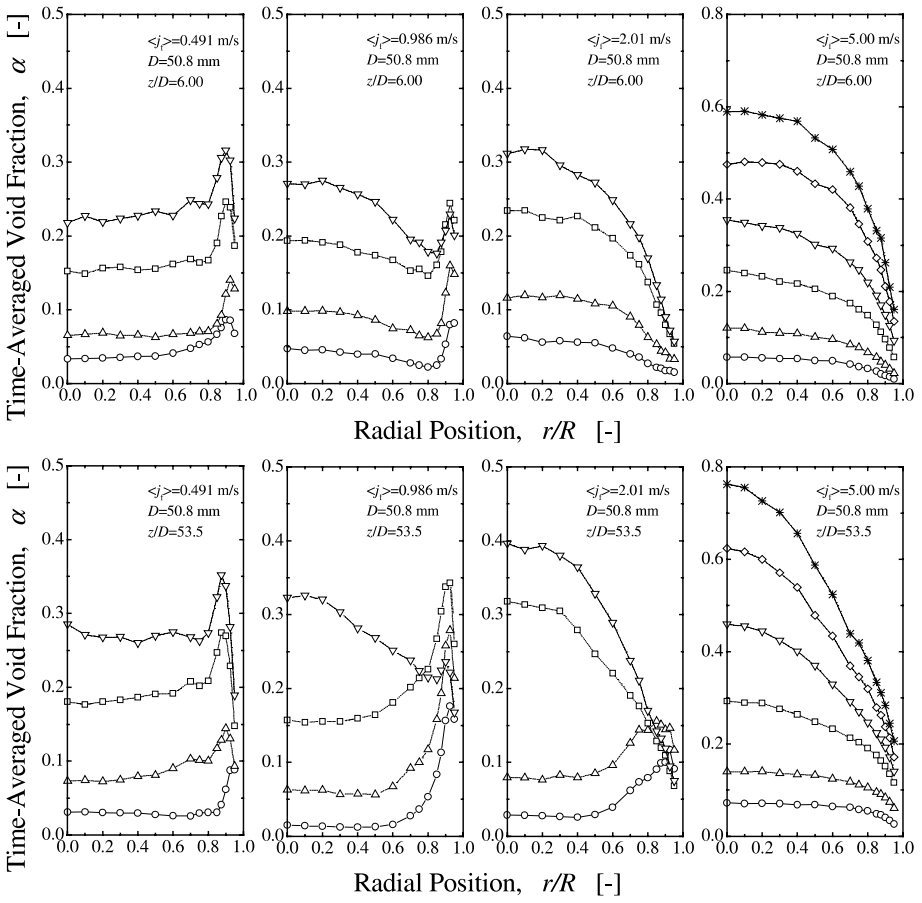

Fig. 5. Axial development of local void fraction profiles [16].

the distribution parameters corresponding to the data shown in Fig. 5. The meanings of the symbols in Figs. 5 and 6 are found in Fig. 6. These figures clearly show the axial development of the void fraction profile as well as the distribution parameter. For example, for $\langle j_f \rangle = 2.01$ m/s and low void fraction region ($\langle \alpha \rangle < 0.15$), as a flow develops, the bubbles migrate from the channel center to the channel wall, resulting in the drastic change from the core peak at $z/D = 6.00$ to the intermediate peak at $z/D = 53.5$. This leads to the axial decrease in the distribution parameter. On the other hand, for $\langle j_f \rangle = 2.01$ m/s and high void fraction region ($\langle \alpha \rangle \geqslant 0.15$), the core peak is pronounced along the axial position, resulting in the axial increase in the distribution parameter. Fig. 7 shows the applicability of Eq. (16) to the developing flows. Eq. (16) can reproduce the dependence of the distribution parameter on the non-dimensional Sauter mean diameter appropriately. A comparison of the model with various experimental data shows a satisfactory agreement. This suggests that Eq. (16) can also be applicable to the developing flows. As shown in Fig. 8, Eq. (19) can also be applicable to the prediction of $\langle D_{Sm} \rangle$ even in the developing flows. However, the average estimation error of $\langle a_i \rangle$ by Eq. (19) increases by $\pm 18.0\%$.

3.5. Verification of constitutive equation for drift velocity given by Ishii

The contribution of the drift velocity to the gas velocity would be rather small for flow regimes such as slug, churn, and annular flow regimes, whereas it would be significant for bubbly flow regime. Thus, it may be important to reevaluate the constitutive equation for the drift velocity in the bubbly flow given by Ishii [4], Eq. (15), with drift velocities determined from measured local flow parameters. Fig. 9 shows the comparison of Eq. (15) with the drift velocities determined from local flow parameters measured in our previous experiments [16,17]. Fig. 10 also shows the comparison of Eq. (15) with the drift velocities by using the databases developed by other investigators [10–13] listed in Table 1. In these figures, the solid and broken lines indicate the calculated drift velocities for bubbly and slug flows, respectively.

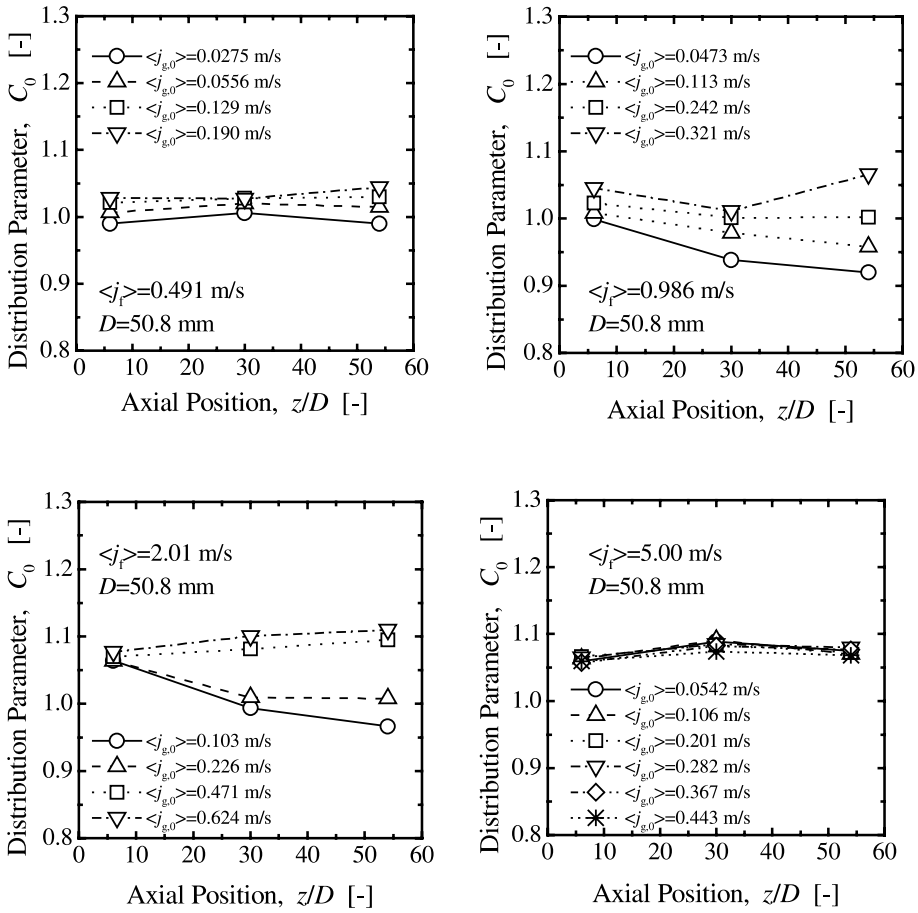

Fig. 6. Axial development of distribution parameters.

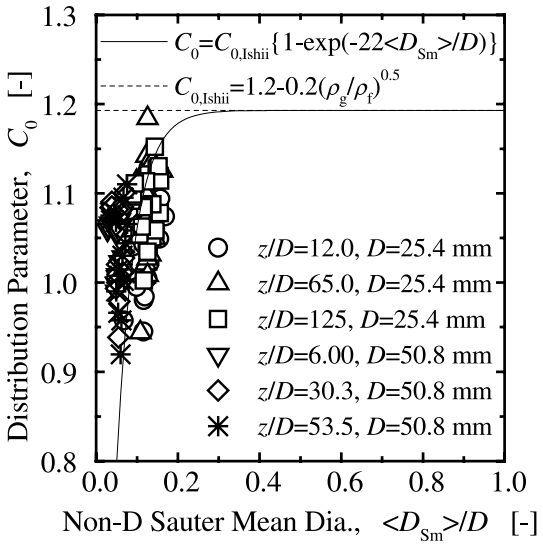

Fig. 7. Comparison of newly developed model for distribution parameter in bubbly flow regime with experimental distribution parameters in developing bubbly flow.

Here, the drift velocity correlation for slug-flow regime is given by Ishii [4] as

$$V_{gj} = 0.35\sqrt{\frac{gD\Delta\rho}{\rho_f}}. \tag{21}$$

The scatter of data points appears to be rather large. As can be seen from Eqs. (1) and (6), the estimation error of the void-fraction-weighted mean drift velocity would mainly be attributed to the measurement error of the relative velocity between phases, which can be calculated by subtracting the liquid velocity from the gas velocity. When the measurement errors for gas and liquid velocities are ±10%, the uncertainty in the void-fraction-weighted mean drift velocity can be roughly estimated to be ±40%, ±80%, and ±400% for the gas velocities of 0.5, 1, and 5 m/s, respectively, from the error propagation. Here, the void-fraction-weighted drift velocity is assumed to be 0.25 m/s in the error estimation by conservative estimate. Thus, it would be very difficult to make a quantitative discussion based on the data for $\langle j_f \rangle \geqslant 1.0$ m/s due to considerably large error.

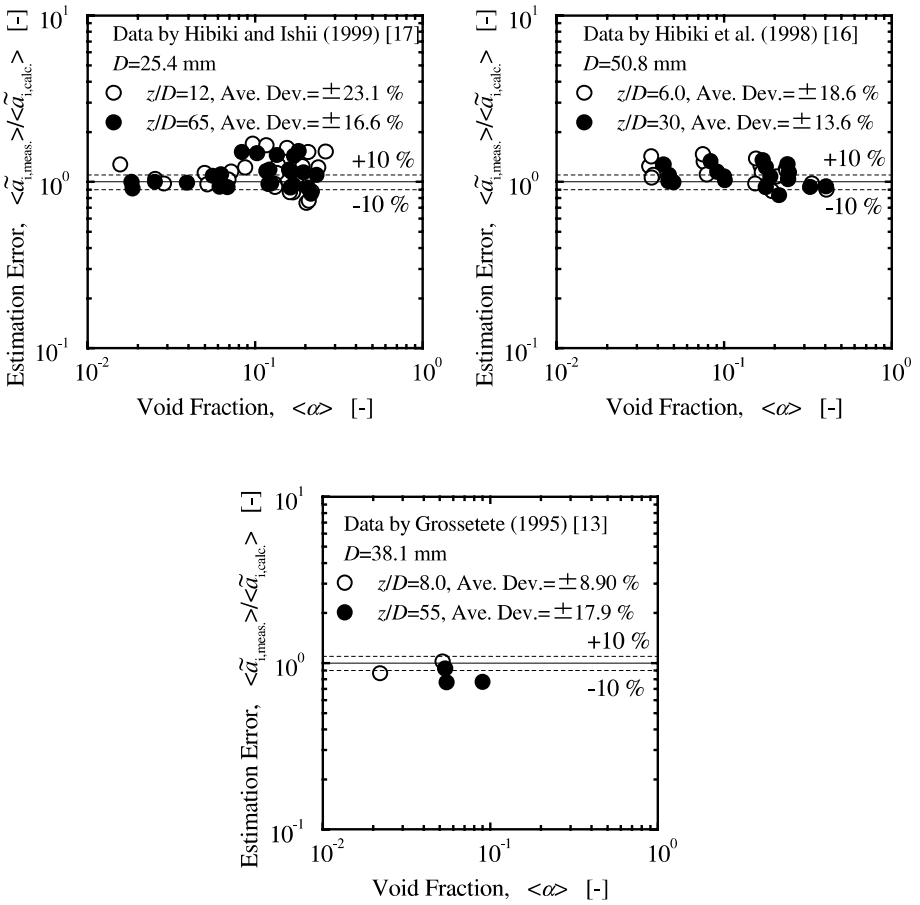

Fig. 8. Applicability of Eq. (19) to developing bubbly flows.

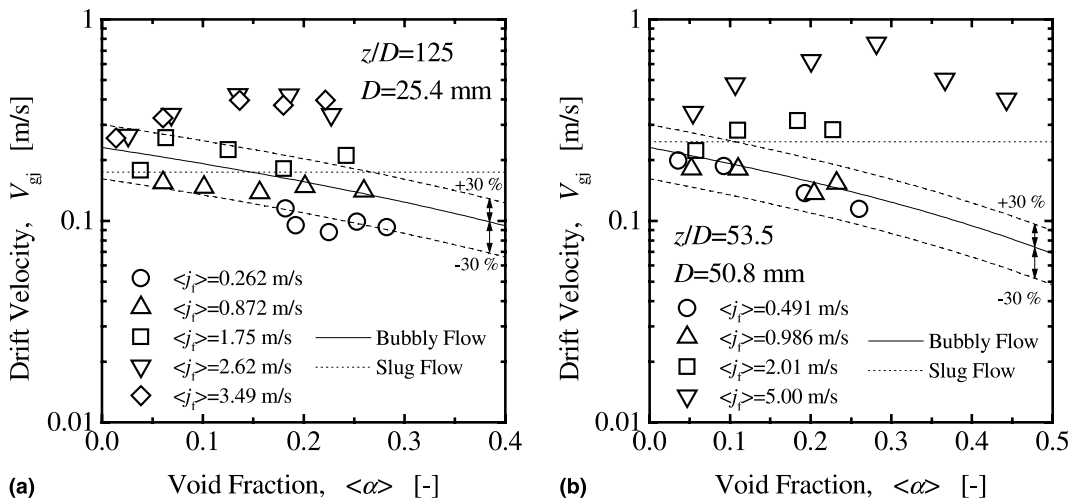

Fig. 9. Comparison of Ishii's model for drift velocity in bubbly flow regime with experimental drift velocities obtained in our previous experiments [16,17]. (a) Experiment using a 25.4 mm-diameter pipe [17], (b) experiment using a 50.8 mm-diameter pipe [16].

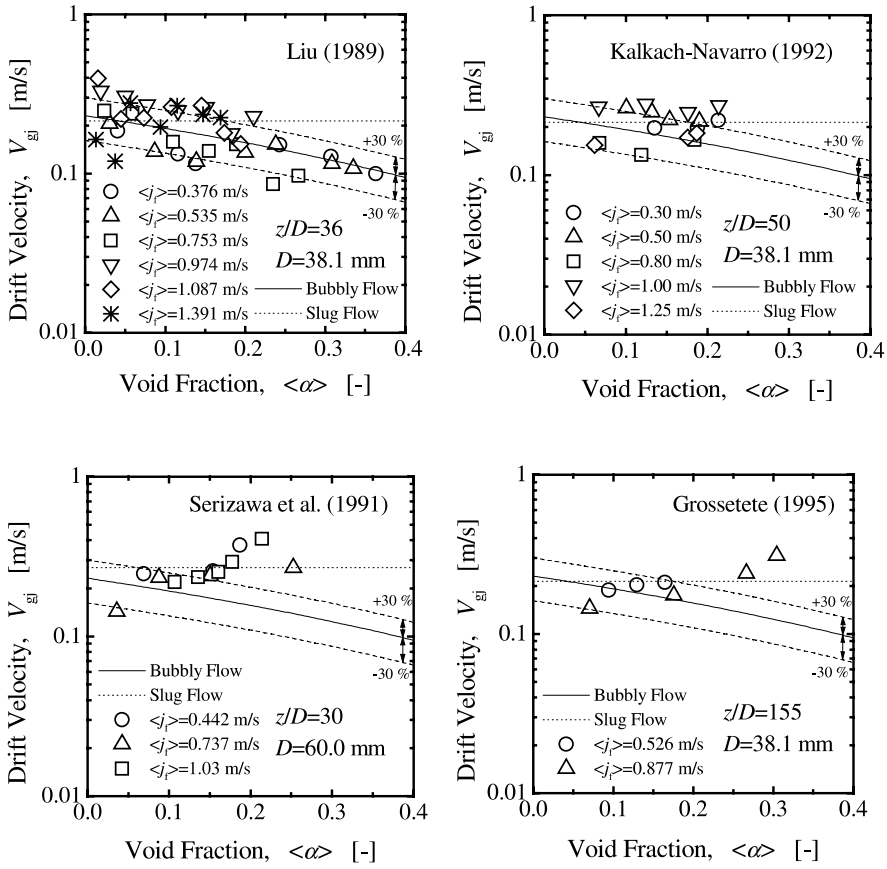

Fig. 10. Comparison of Ishii's model for drift velocity in bubbly flow regime with experimental drift velocities obtained by various investigators [10–13].

As can be clearly seen from Figs. 9 and 10, the void-fraction-weighted mean drift velocity appears to decrease with the increase in void fraction. The drift velocity correlation developed by Ishii [4], Eq. (15), can represent this tendency marvelously. For $\langle\alpha\rangle \geqslant 0.15$, some data sets agree with the drift velocity calculated by Eq. (21) rather than Eq. (15). This may be attributed to the flow regime transition from bubbly flow to slug flow. Taking account of large error in experimental drift velocity, it can be concluded that Eq. (15) can give the proper trend of the drift velocity in bubbly flow regime against the void fraction as well as good predictions of the values of the drift velocities in bubbly flow regime.

Unfortunately, for high mixture volumetric fluxes ($\triangledown, \diamondsuit$ in Fig. 9(a), $\square, \triangledown$ in Fig. 9(b)) the validity of Eq. (15) cannot be proven by the present databases due to considerably large error in the experimental void-fraction-weighted mean drift velocity. However, for the high mixture volumetric fluxes, the local slip effect is negligibly small as compared with the distribution parameter effect. Thus, in calculating a void-fraction-weighted mean gas velocity, the value of the void-fraction-weighted mean drift velocity is not critical.

3.6. Axial development of drift velocity

Fig. 11 shows examples of the axial development of the drift velocities obtained in our previous experiment using a pipe with $D = 50.8$ mm [16]. The upper figures are the axial development of the drift velocities for $\langle j_f\rangle = 0.491$ and 0.986 m/s. The figures at the lower left and right show the dependence of the drift velocity on the void fraction obtained at $z/D = 6.00$ and 30.3, respectively. The dependence obtained at $z/D = 53.5$ is also found in Fig. 9(b). It can be seen from the lower figures in Fig. 11 that Eq. (15) gives good predictions of the values of the drift velocities for low liquid-velocity region ($\bigcirc, \triangle$) at $z/D = 6.00$ and 30.3. The upper figures show that the drift velocity appears to be already developed even at the first measuring station, $z/D = 6.00$. Thus, it may be concluded that Eq. (15) can be applicable to a developing flow except for the flow very near the inlet.

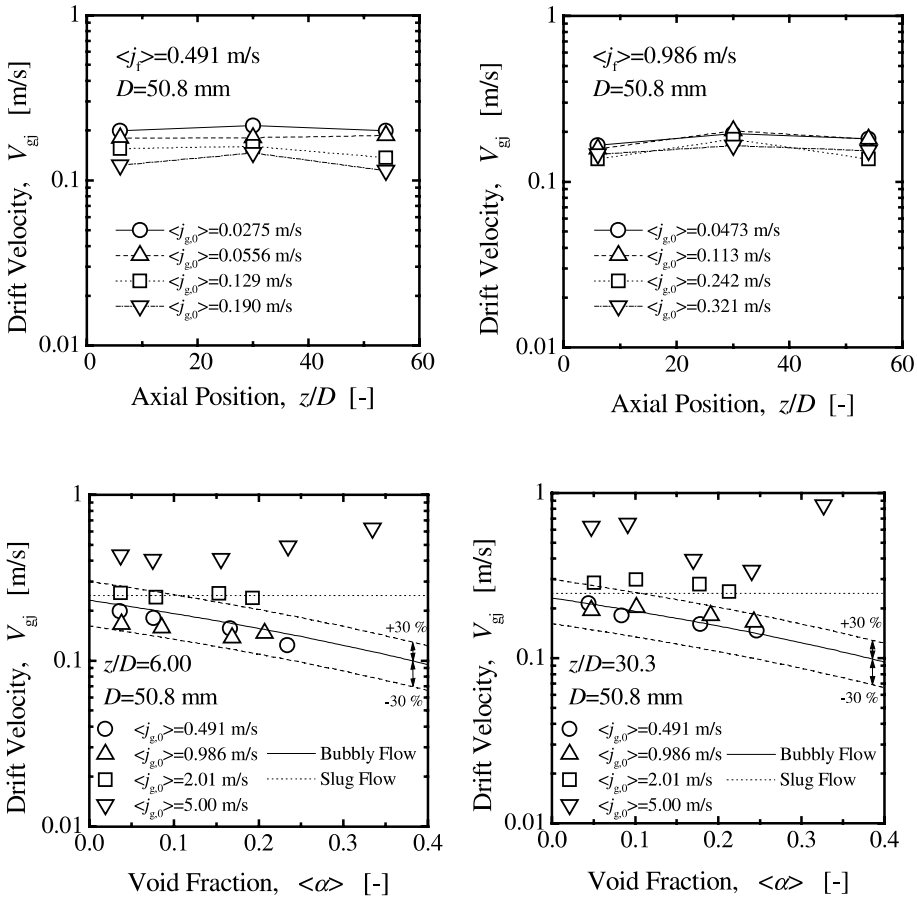

Fig. 11. Axial development of drift velocities.

4. Conclusions

In view of the practical importance of the drift-flux model for two-phase flow analysis in general and in the analysis of nuclear-reactor transients and accidents in particular, the distribution parameter and the drift velocity have been studied for bubbly flow regime. The obtained results are as follows:

1. The constitutive equation, Eq. (16), that specifies the distribution parameter in the bubbly flow has been derived by taking into account the effect of the bubble size on the phase distribution, since the bubble size would govern the distribution of the void fraction.
2. A comparison of newly developed constitutive equation for the distribution parameter, Eq. (16), with various fully developed bubbly flow data over a wide range of flow parameters shows a satisfactory agreement. It has also been confirmed experimentally that the newly developed equation can be applicable to developing bubbly flows.
3. The constitutive equation for the drift velocity developed by Ishii, Eq. (15), has been validated by the drift velocity calculated directly by local flow parameters such as void fraction, gas velocity and liquid velocity measured under steady fully developed bubbly flow condition. It has also been confirmed experimentally that Ishii's equation can be applicable to developing bubbly flows.

Acknowledgements

This work was performed under the auspices of the US Department of Energy's Office of Basic Energy Science. The authors would like to express their sincere appreciation for the encouragement, support and technical comments on this program from Drs. Manley, Goulard, and Price of DOE/BES.

References

[1] J.M. Delhaye, Equations fondamentales des écoulements diphasiques, Part 1 and 2, CEA-R-3429, France, 1968.

[2] M. Ishii, Thermo-fluid Dynamic Theory of Two-phase Flow, Eyrolles, Paris, 1975.
[3] N. Zuber, J.A. Findlay, Average volumetric concentration in two-phase flow systems, J. Heat Transfer 87 (1965) 453–468.
[4] M. Ishii, One-dimensional drift-flux model and constitutive equations for relative motion between phases in various two-phase flow regimes, ANL-77-47, USA, 1977.
[5] Atomic Energy Society of Japan, Division of Thermal-hydraulics (Eds.), Numerical Analysis of Gas-Liquid Two-phase Flow, Asakura, Japan, 1993, in Japanese.
[6] Y. Hirao, K. Kawanishi, A. Tsuge, T. Kohriyama, Experimental study on drift flux correlation formulas for two-phase flow in large diameter tubes, in: Proceedings of the second International Topical Meeting on Nuclear Power Plant Thermal Hydraulics and Operations, Tokyo, Japan, 1986, pp. 1-88–1-94.
[7] I. Kataoka, M. Ishii, Drift flux model for large diameter pipe and new correlation for pool void fraction, Int. J. Heat Mass Transfer 30 (1987) 1927–1939.
[8] I. Kataoka, M. Ishii, A. Serizawa, Local formulation and measurements of interfacial area concentration in two-phase flow, Int. J. Multiphase Flow 12 (1984) 505–529.
[9] A. Serizawa, I. Kataoka, I. Michiyoshi, Turbulence structure of air–water bubbly flow – I. Measuring techniques, Int. J. Multiphase Flow 2 (1975) 221–233.
[10] T.J. Liu, Experimental investigation of turbulence structure in two-phase bubbly flow, Ph.D. Thesis, Northwestern University, USA, 1989.
[11] A. Serizawa, I. Kataoka, I. Michiyoshi, Phase distribution in bubbly flow, in: G.F. Hewitt, J.M. Delhaye, N. Zuber (Eds.), Multiphase Science and Technology, vol. 6, Hemisphere, Washington, DC, 1991, pp. 257–301.
[12] S. Kalkach-Navarro, The mathematical modeling of flow regime transition in bubbly two-phase flow, Ph.D. Thesis, Rensselaer Polytechnic Institute, USA, 1992.
[13] C. Grossetete, Caracterisation experimentale et simulations de l'evolution d'un ecoulement diphasique a bulles ascendant dans une conduite verticale, Ph.D. Thesis, Ecole Centrale Paris, France, 1995.
[14] S. Hogsett, M. Ishii, Local two-phase flow measurements using sensor techniques, Nucl. Eng. Des. 175 (1997) 15–24.
[15] T. Hibiki, S. Hogsett, M. Ishii, Local measurement of interfacial area, interfacial velocity and liquid turbulence in two-phase flow, Nucl. Eng. Des. 184 (1998) 287–304.
[16] T. Hibiki, M. Ishii, Z. Xiao, Axial interfacial area transport of vertical bubbly flows, Int. J. Heat Mass Transfer 44 (2001) 1869–1888.
[17] T. Hibiki, M. Ishii, Experimental study on interfacial area transport in bubbly two-phase flows, Int. J. Heat Mass Transfer 42 (1999) 3019–3035.
[18] S.T. Revankar, M. Ishii, Local interfacial area measurement in bubbly flow, Int. J. Heat Mass Transfer 35 (1992) 913–925.
[19] A. Serizawa, I. Kataoka, Phase distribution in two-phase flow, in: N.H. Afgan (Ed.), Transient Phenomena in Multiphase Flow, Hemisphere, Washington, DC, 1988, pp. 179–224.
[20] Y. Taitel, D. Bornea, E.A. Dukler, Modelling flow pattern transitions for steady upward gas–liquid flow in vertical tubes, AIChE J. 26 (1980) 345–354.
[21] K. Sekoguchi, T. Sato, T. Honda, Two-phase bubble flow (first report), Trans. JSME 40 (1974) 1395–1403 (in Japanese).
[22] I. Zun, Transition from wall void peaking to core void peaking in turbulent bubbly flow, in: N.H. Afgan (Ed.), Transient Phenomena in Multiphase Flow, Hemisphere, Washington, DC, 1988, pp. 225–245.
[23] A. Tomiyama, A. Sou, I. Zun, N. Kanami, T. Sakaguchi, Effect of Eötvös number and dimensionless liquid volumetric flux on lateral motion of a bubble in a laminar duct flow, in: Proceedings of the 2nd International Conference on Multiphase Flow '95 Kyoto, Kyoto, Japan, 1995, pp. PD1-11–PD1-18.
[24] I. Kataoka, M. Ishii, Mechanism and correlation of droplet entrainment and deposition in annular two-phase flow, ANL-82-44, USA, 1983.
[25] N.N. Clark, J.W. Van Egmond, E.P. Nebiolo, The drift-flux model applied to bubble columns and low velocity flows, Int. J. Multiphase Flow 16 (1990) 261–279.
[26] T. Hibiki, M. Ishii, Experimental study on hot-leg U-bend two-phase natural circulation in a loop with a large diameter pipe, Nucl. Eng. Des. 195 (2000) 69–84.
[27] T. Hibiki, M. Ishii, Effect of inlet geometry on hot-leg U-bend two-phase natural circulation in a loop with a large diameter pipe, Nucl. Eng. Des. 203 (2001) 209–228.
[28] T. Hibiki, M. Ishii, Interfacial area concentration in steady fully-developed bubbly flow, Int. J. Heat Mass Transfer 44 (2001) 3443–3461.
[29] G. Kocamustafaogullari, W.D. Huang, J. Razi, Measurement of modeling of average void fraction, bubble size and interfacial area, Nucl. Eng. Des. 148 (1994) 437–453.
[30] T. Hibiki, M. Ishii, One-group interfacial area transport of bubbly flows in vertical round tubes, Int. J. Heat Mass Transfer 43 (2000) 2711–2726.
[31] R.W. Lockhart, R.C. Martinelli, Proposed correlation of data for isothermal two-phase, two-component flow in pipes, Chem. Eng. Prog. 5 (1949) 39–48.